Electronic Supplementary Material (ESI) for Materials Chemistry Frontiers.

Supporting Information

Anchoring 1T/2H MoS_2 nanosheets on carbon nanofibers containing Si nanoparticles as a flexible anode for lithium-ion batteries

Xianping Du[a], Ying Huang[a]*, Zhenhe Feng[b], Jiaming Wang[a], Zhiliang Duan[a], Xu Sun[c]*

[a] *MOE Key Laboratory of Material Physics and Chemistry under Extraordinary Conditions, School of Chemistry and Chemical Engineering, Northwestern Polytechnical University, Xi'an 710072, PR China*
[b] *Shanghai Institute of Space Power-Sources, Shanghai 200245, PR China*
[c] *Ningbo Institute of Northwestern Polytechnical University, Ningbo 315103, PR China*

*Corresponding author.
Email addresses: yingh@nwpu.edu.cn (Y. Huang); sunxu@nwpu.edu.cn (X. Sun).

*Corresponding author.
Email addresses: yingh@nwpu.edu.cn (Y. Huang), sunxu@nwpu.edu.cn (X. Sun)

1. Experimental

1.1. Synthesis of materials

polyacrylonitrile (PAN, Mw = 150000) was purchased from Sigma. Si nanoparticles were purchased from the corporation of Macklin, which were synthesized using the plasma technology. N, N-dimethylformamide (DMF, 99.9%), ammonium molybdate ($(NH_4)_6Mo_7O_{24}\cdot H_2O$), thiourea ($CH_3CSNH_2$), ammonium bicarbonate (NH_4HCO_3). All reagents can be used directly without further purification.

1.2. Materials characterization

The crystalline property of the obtained samples was analyzed by X-ray powder diffraction (XRD, Rigaku, Cu-Ka) with a scan rate of 4 ℃/min. The morphology and structure of samples were observed by scanning electron microscopy (SEM, Verios G4, USA)) and field emission transmission electron microscope (FETEM, FEI Talos F200X). X-ray Photoelectron Spectroscopy (XPS, Kratos, USA) could be used to reveal the surface elements of the samples. Raman spectrophotometer (Alpha 300R) was employed to further determine the composition and phase structures of the final product. In order to measure the Si content of the Si@CNFs and Si@CNFs@1T/2H MoS_2 electrodes, thermal gravimetric analysis (TGA) (Model Q50, TA, USA) were performed from 30 to 1000 ℃ at the heating rate of 10 ℃/min in air atmosphere.

1.3. Electrochemical characterization

The obtained thin films were directly conducted as the working electrode and the lithium foil as the counter electrode to assemble CR2016 coin-type cells in an argon-filled glove box. The Si anodes were prepared through coating a homogeneous slurry

consisting of commercial Si nanoparticles, acetylene black and PVDF under a weight ratio of 7 : 2 : 1 on copper foil. The electrolyte was 1M $LiPF_6$ in a mixture of ethylene carbonate (EC)/diethyl carbonate (DEC)/dimethyl carbonate (DMC) (1 : 1 : 1 in volume ratio) with the additive of 6 wt% fluoroethylene carbonate (FEC). Electrochemical measurements were performed at the multi-channel current static system Land (LAND CT200IA). Cyclic voltammetry and electrochemical impedance spectroscopy of batteries were measured through electrochemical workstation (Autolab, PGSTAT302 N). Furthermore, the four-point probe was used for the conductivity measurement of the samples (RTS-8, 4 Points Tech, China). Furthermore, the full-cell was fabricated employing the Si@CNFs@1T/2H MoS_2 anode and the commercially available $LiFePO_4$ (LFP) cathode. The LFP cathode was prepared using a traditional electrode preparation process. The slurry consisted of LFP, poly(vinylidene fluoride) (PVDF), acetylene black with a weight ratio of 8 : 1 : 1, which was cast onto an aluminum foil and dried at 80 °C under vacuum for 12 h. For the full-cell test, the Si@CNFs@1T/2H MoS_2 electrode was pre-lithiated in the half-cell for three cycles at the current density of 200 mA g^{-1} to reduce the lithium loss and form a stsble SEI film. The cycling performance of the Si@CNFs@1T/2H MoS_2//LFP full-cell was performed under the voltage window of 0.01-3.7 V.

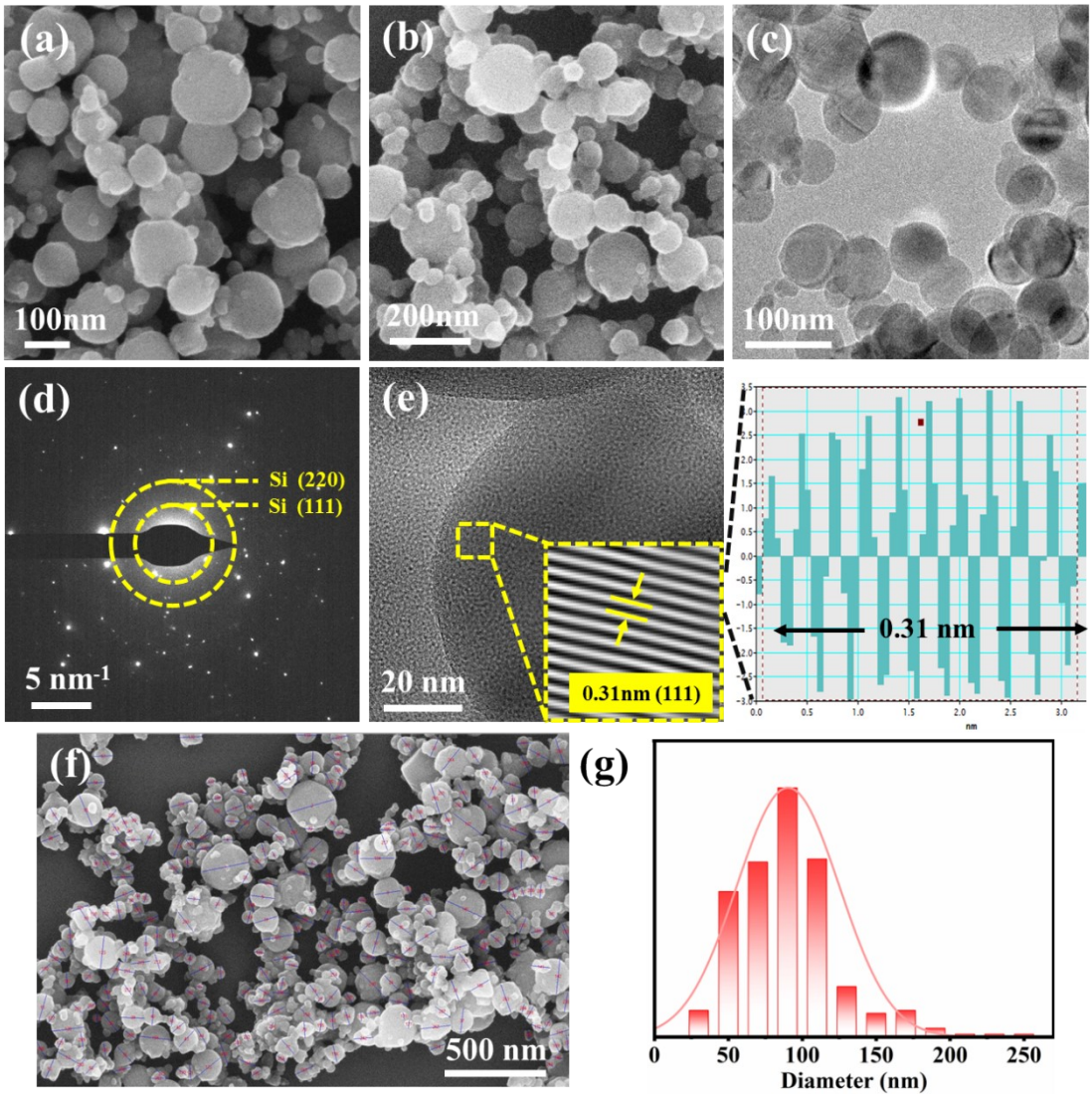

Fig. S1. SEM images of Si NPs (a, b); TEM image of Si NPs (c); SAED pattern of Si NPs (d); HRTEM image of Si NPs (e); Nano Measurer software to analyze the particle size of Si NPs (f), Size distribution pattern of Si NPs (g).

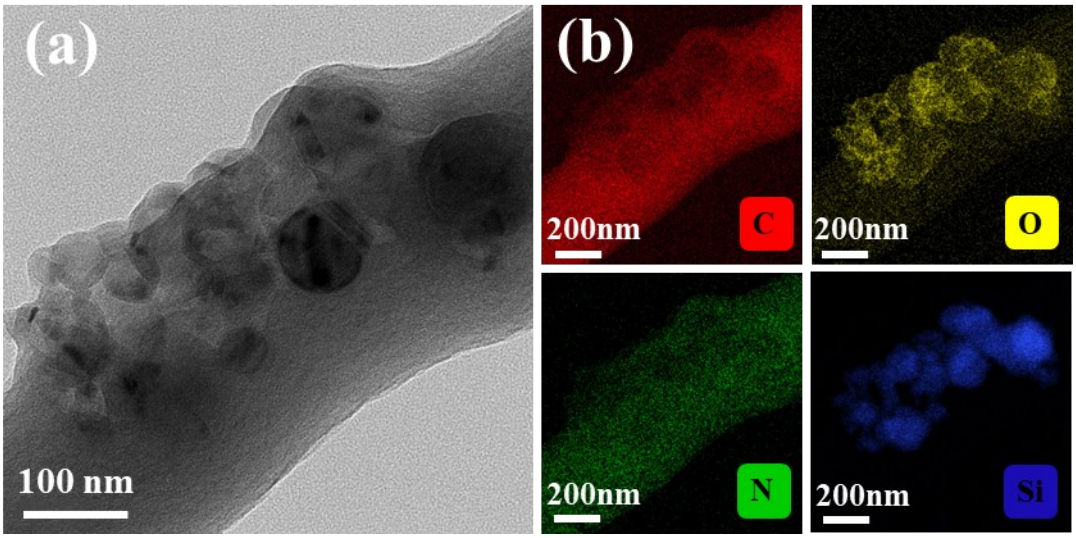

Fig. S2. TEM image of Si@CNFs (a); EDS mappings of Si@CNFs (b).

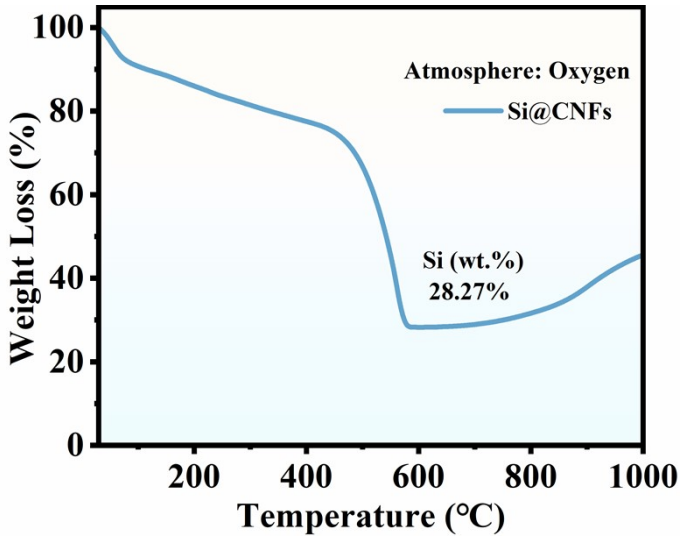

Fig. S3. TGA curves of the Si@CNFs electrodes under air atmosphere.

Table S1. The weight of the Si@CNFs and Si@CNFs@1T/2H MoS_2 electrodes

Number	Si@CNFs (g)	Si@CNFs@1T/2H MoS_2 (g)	Si content in Si@CNFs@1T/2H MoS_2
1	0.0029	0.0064	12.81%
2	0.0022	0.0042	14.81%
3	0.0033	0.0068	13.72%
4	0.0027	0.0069	11.06%
5	0.0030	0.0075	11.31%
6	0.0057	0.0140	11.51%
	Average		12.56%

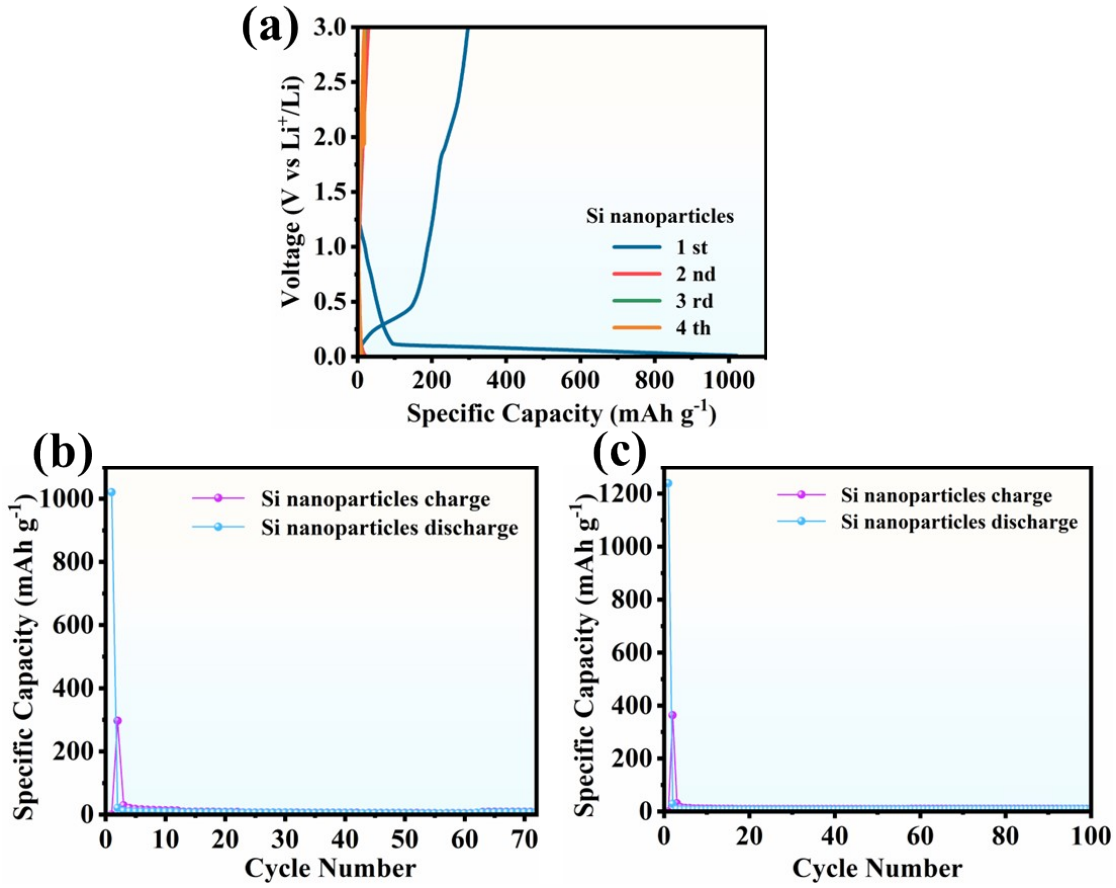

Fig. S4. First four charge-discharge of Si anode (a); rate performance of Si anode at the different current densities (b); cycling performance of Si anode at the current density of 100mA g^{-1} (c).

Table S2. The fitted values of the EIS curves in Fig. 5d.

Materials	Rs (Ω)	Rct (Ω)
Si@CNFs	1.256	88.09
Si@CNFs@1T/2H MoS_2	0.80446	22.15

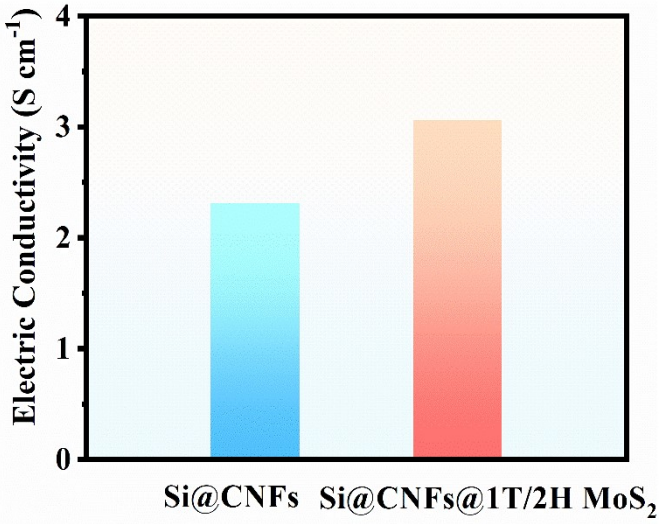

Fig. S5. The conductivity of Si@CNFs and Si@CNFs@1T/2H MoS_2 electrodes.

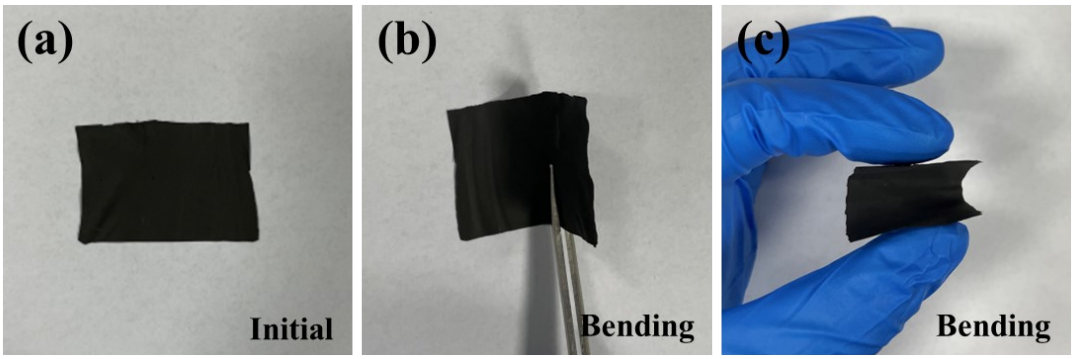

Fig. S6. Images of the flexible characteristic of Si@CNFs@1T/2H MoS_2 paper.

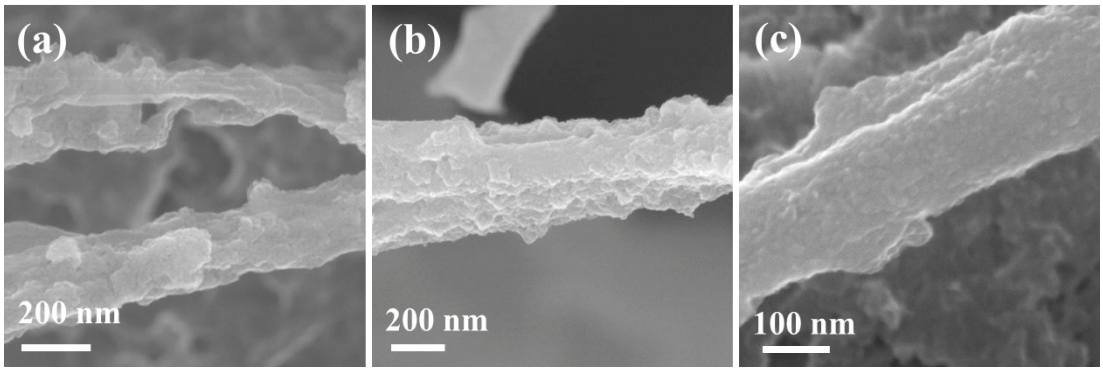

Fig. S7. SEM image of the Si@CNFs@1T/2H MoS_2 electrodes after cycling (a-c)

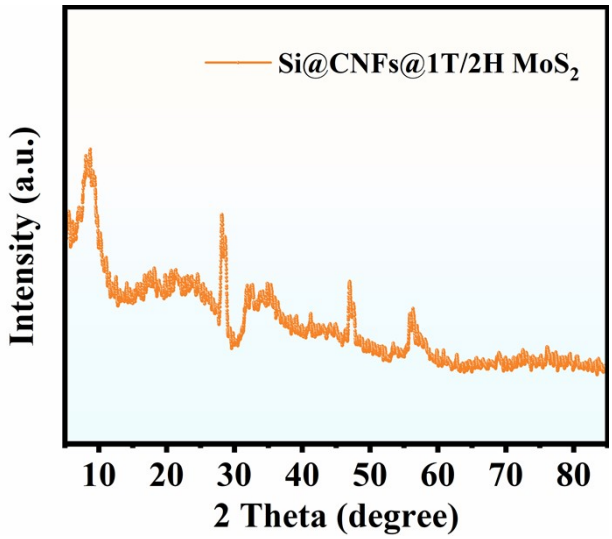

Fig. S8. XRD pattern of the Si@CNFs@1T/2H MoS_2 electrode after cycling

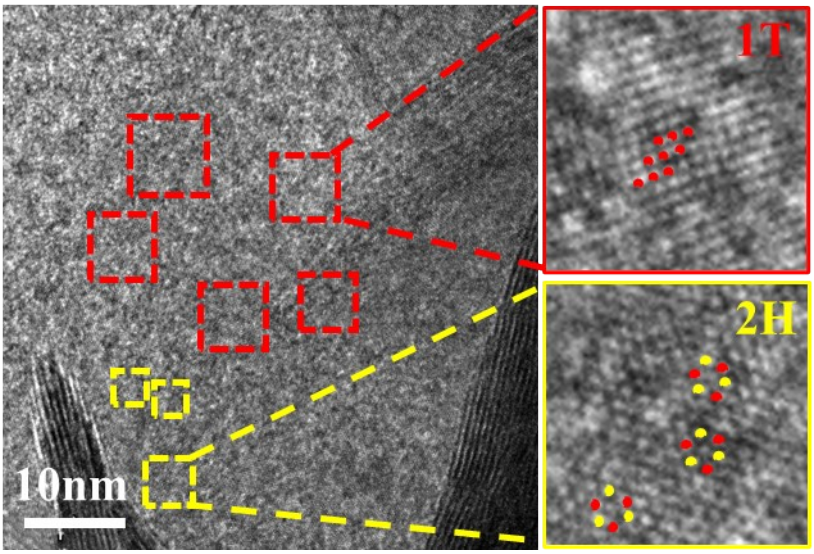

Fig. S9. HRTEM image of the Si@CNFs@1T/2H MoS_2 electrode after cycling

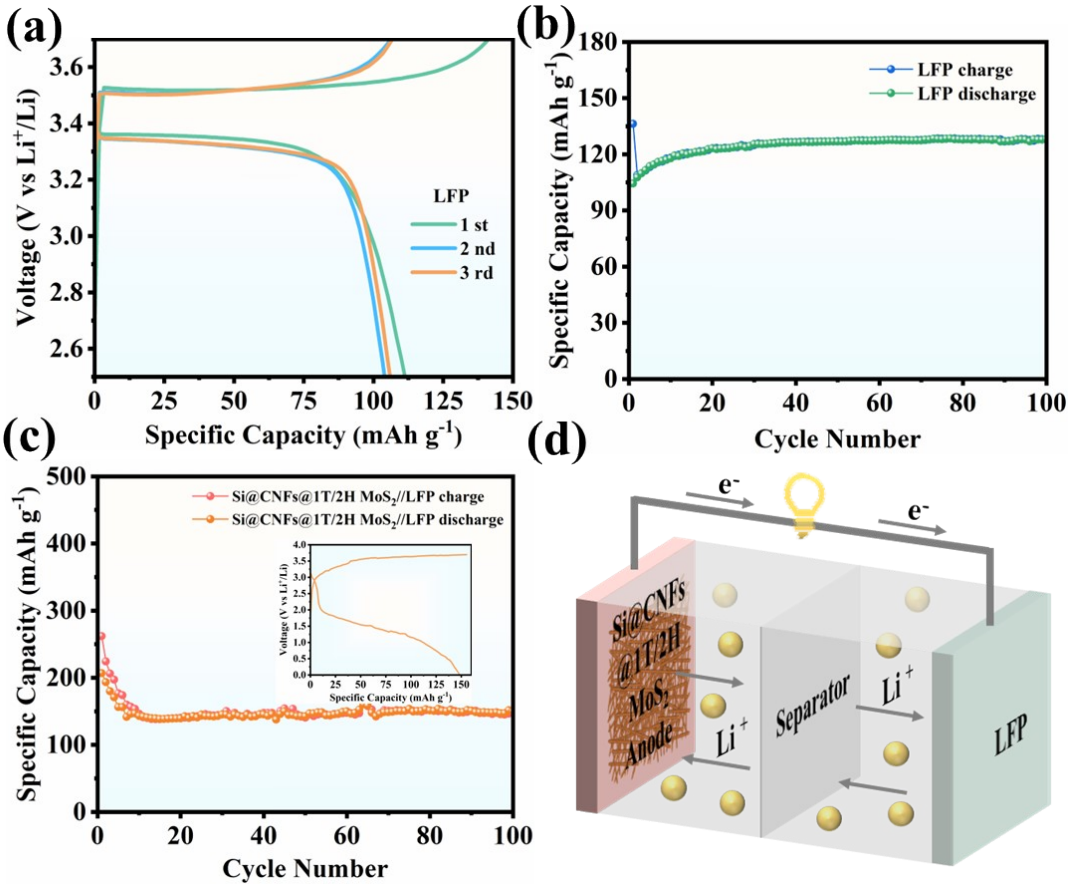

Fig. S10. first three charge-discharge curves (a) and cycling performance (b) of the LFP half-cell; the cycling performance of the Si@CNFs@1T/2H MoS_2//LFP full-cell with the corresponding charge/discharge profiles showing in the inset (c); the mechanism figure of the Si@CNFs@1T/2H MoS_2//LFP full-cell during the cycling (d).